Signal Transduction in the Photoactive Yellow Protein. I. Photon Absorption and the Isomerization of the Chromophore

Gerrit Groenhof,[1] Marc F. Lensink,[2] Herman J. C. Berendsen,[1] Jaap G. Snijders,[3] and Alan E. Mark[1*]

[1]*Department of Biophysical Chemistry, Groningen Biomolecular Sciences and Biotechnology Institute, Rijksuniversiteit Groningen, Groningen, The Netherlands*
[2]*Department of Biochemistry, the University of Oulu, Oulu, Finland*
[3]*Department of Theoretical Chemistry, Materials Science Centre, Rijksuniversiteit Groningen, Groningen, The Netherlands*

ABSTRACT **Molecular dynamics simulation techniques together with time-dependent density functional theory calculations have been used to investigate the effect of photon absorption by a 4-hydroxy-cinnamic acid chromophore on the structural properties of the photoactive yellow protein (PYP) from *Ectothiorodospira halophila*. The calculations suggest that the protein not only modifies the absorption spectrum of the chromophore but also regulates the subsequent isomerization of the chromophore by stabilizing the isomerization transition state. Although signaling from PYP is thought to involve partial unfolding of the protein, the mechanical effects accompanying isomerization do not appear to directly destabilize the protein. Proteins 2002;48:202–211.** © 2002 Wiley-Liss, Inc.**

INTRODUCTION

Ectothiorodospira halophila, a small salt-tolerant bacterium, avoids excessive exposure to harmful ultraviolet radiation by detecting blue light and moving in a direction opposite to the gradient.[1] The cytoplasm of *E. halophila* contains a small water-soluble protein, named photoactive yellow protein (PYP), that has an absorption maximum that closely matches the action spectrum for the negative phototaxis. Therefore, PYP has been proposed to be the primary photoreceptor for this biologic process. PYP also serves as a structural prototype for the widely distributed Per–Arnt–Sim (PAS) class of signal transduction proteins.[2]

PYP contains a 4-hydroxy-cinnamic acid (or *p*-coumaric acid) chromophore linked covalently to the γ-sulfur of Cys69 via a thioester bond (Fig. 1).[3] The chromophore is completely buried within a hydrophobic pocket with no exposure to solvent. The apolar environment lowers the pK_a of the chromophore's phenolic group to such an extent that this group is deprotonated at pH = 7.0. The resulting net negative charge on the phenolic oxygen atom is stabilized by a hydrogen bonding network formed between this oxygen atom and the hydroxyl groups of three nearby

amino acid side-chains [Tyr42, Glu46, and Thr50; Fig. 1.(b)].[4] The negative charge is further stabilized by charge delocalization over the chromophore via the conjugated p$_z$ orbitals. Due to its interactions with nearby amino acid residues, the bound chromophore absorbs photons of blue light (λ_{max} = 446 nm), giving the protein its characteristic yellow color.

Upon absorbing a photon, PYP enters a reversible photocycle, depicted in Fig. 2. At room temperature, four distinct intermediate states can be identified along the cycle. The state described in the previous paragraph is the resting or ground state in the cycle, denoted by pG. In this state, the protein can be activated by absorbing a photon. The absorption of a photon triggers a *trans*-to-*cis* isomerization of the double bond in the chromophore [bond *b*, Fig. 1(a)] within a few nanoseconds.[5,6] Infrared spectroscopy has shown that during the isomerization process the hydrogen-bonding network, which stabilized the deprotonated chromophore in the ground state,[7] remains intact. After photoisomerization, the protein is in the red-shifted state, denoted by pR. This name reflects the observed redshift in the absorption frequencies with respect to the ground state.

Over a period of microseconds, the protein then partially unfolds, leading to the blue-shifted state, in which the unfolding is at a maximum.[8,9] The blue-shifted state, denoted by pB, is believed to be the activated or signaling state. During the unfolding process, the phenolate group of the chromophore becomes protonated. This leads to a higher electronic stability of the chromophore and hence to a blueshift in the absorption frequencies. The precise order of the events that lead to this intermediate state is not known.

After the blue-shifted state, the protein completes the final stage of the cycle. The protein slowly refolds, the chromophore reisomerizes and loses its proton, and the system is restored to its equilibrium state, the ground

*Correspondence to: Alan E. Mark, Department of Biophysical Chemistry, Groningen Biomolecular Sciences and Biotechnology Institute, Rijks universiteit Groningen, Nijenborgh 4, 9747 AG Groningen, The Netherlands. E-mail: a.e.mark@chem.rug.nl
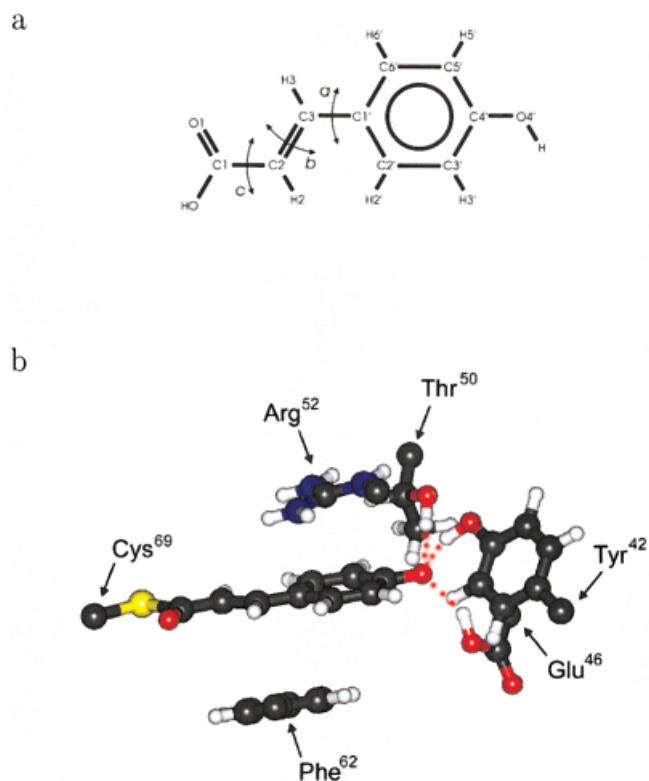
Fig. 1. 4-Hydroxy-cinnamic acid (or *p*-coumaric acid) chromophore: (**a**) free and (**b**) bound to PYP. In the protein, the chromophore is covalently linked to Cys[69]. Its phenolic acid group is deprotonated but stabilized by hydrogen-bonding interactions with nearby side-chains.
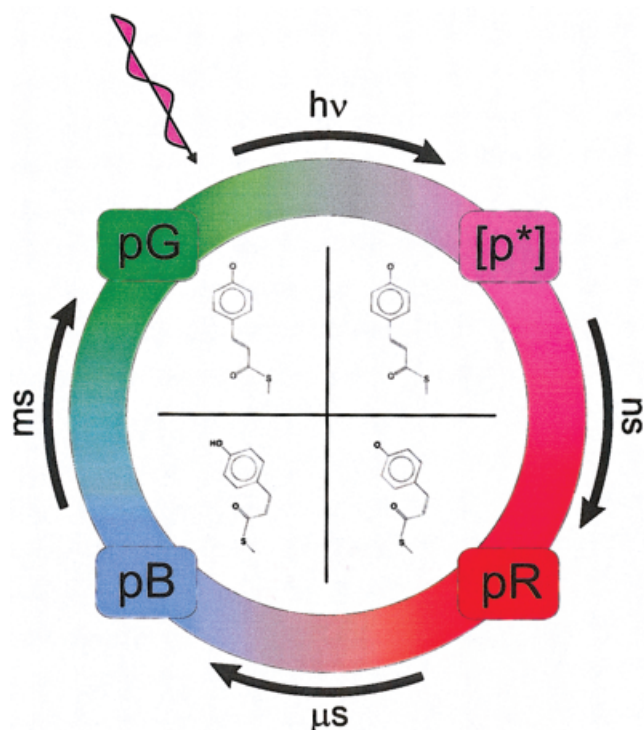

Fig. 2. Photocycle of PYP. Inside the cycle, the conformations of the chromophore in the different stages are drawn. An absorption of a photon in the ground state (pG) leads to the excited state ([p*]). Isomerization of the chromophore leads to the next intermediate state, the so-called red-shifted state ([pR]). Subsequently, the protein undergoes large conformational changes and the phenolate group of the chromophore becomes protonated to give the blue-shifted state ([pB]). In the last stage of the cycle, the chromophore reisomerizes and the protein folds back to the ground state (pG).

state. Because the timescale on which these final processes occur is in the order of milliseconds, the third stage is most likely thermally driven.

Using different computational techniques, we investigated the first three stages of the photocycle. The goal was to shed light on the mechanism by which PYP detects blue light and passes on the signal to a second messenger. This article focuses on the first two stages of the cycle, namely, photon absorption and the subsequent isomerization. A second article is dedicated to the third stage, in which PYP undergoes major conformational changes.

To investigate the photon absorption process, we performed a number of time-dependent density functional theory (TDDFT) computations.[10,11] TDDFT provides an efficient means to calculate the first-order linear response of the electronic density to a time-dependent electric field. Because photoexcitation is essentially an interplay between the electronic component of electromagnetic radiation and the polarizability (i.e., linear response of the electrons) of the molecule, TDDFT is a useful technique for calculating optical response properties of molecules, such as excitation frequencies and transition dipole moments. For a more detailed description of the TDDFT method, see the excellent review of Gross and Kohn.[12]

Photon absorption is believed to trigger a rapid isomerization of the chromophore. In an attempt to study this process at the atomic level, we performed molecular dynamics (MD) simulations of PYP. In a MD simulation, New-

ton's equations of motion are integrated in time for all atoms in a system.[13,14] In this way, one can model the time evolution of the system and obtain a description of the dynamics of the system at an atomic level. With the current state of computer technology, the maximum timescale that can be reached in a classic simulation of a small protein ($\approx$ 20,000 atoms) is in the order of 10–100 ns. Therefore, MD is limited to relatively fast processes. Isomerization is rapid, and in principle MD is very suitable for studying it. However, due to the cost of the TDDFT calculations it was not possible to directly simulate the dynamics of the system in the excited state nor the process of relaxation back to the ground state in detail. Instead, the process was mimicked by modifying the ground-state potential functions to model the excited state (p*). The system was then allowed to evolve before the ground-state potential functions were reapplied. Although crude, this approach can be justified based on the outcome of the TDDFT computations and has allowed us to study the structural and electronic reorganization within the protein that accompany photoisomerization

MATERIALS AND METHODS
Excitation Calculations

The excitation energies were calculated using the TD-DFT routines[11,15] of the Amsterdam Density Functional

(ADF 99) program.[10] The structures of the chromophore used in the TDDFT calculations are shown in Figure 1. The structure in Figure 1(a) was used to investigate the absorption characteristics of the chromophore in vacuo. The cysteine side chain (Cys69) is cut at the C_α–C_β bond and capped with a hydrogen atom. To study the influence of the PYP environment on the properties of the chromophore, a larger calculation was performed in which the surroundings of the chromophore inside PYP were also taken into account. The structure used in these calculations is shown in Figure 1(b). All 74 atoms of this structure were explicitly treated in the TDDFT calculations. The positions of these atoms were averaged over 6 ns of the pG simulation (see below). Again, the bonds between the C_α and C_β atoms of each residue were broken and capped with hydrogens. In all TDDFT calculations, the Volko–Wilk–Nusair local density functional was used together with the Becke–Perdew density gradient correction. A triple-zeta basis set of Slater-type functions, with two added polarization functions, was used (basis set V of the ADF package, which is the highest basis set available within ADF 99). This basis set is well balanced and other studies have indicated that it should be sufficiently complete for our purposes[16]. For the calculation of a small part of the excited-state potential energy surface in vacuo, a number of chromophore conformations was generated by systematically changing the four dihedral angles (*a, b, c,* and *d* in Fig. 1) in the tail of the chromophore in steps of 2.5°. An excitation calculation was then performed for each conformation. The same procedure was carried out for computing the isomerization profiles for the isomerization reaction observed in the *p** simulation. In this case, however, the conformations of the chromophore were taken from successive frames of that simulation.

MD Simulations

Initially, PYP was simulated for 6 ns in the ground state. The starting coordinates for this simulation, denoted as pG, were taken from the high-resolution X-ray structure[4] (entry 2PHY of the Protein Data Bank). Five simulations were started from alternating frames of the pG simulation. In these simulations, the ground-state partial atomic charges of the chromophore were replaced by excited-state partial charges. In addition, the potential functions describing the rotation of the dihedrals in the tail of the chromophore (*a, b, c,* and *d* in Fig. 1), which model the potential energy as a function of dihedral angle, were removed. The simulations, denoted as barrier-less or p*, were performed to investigate the short-term effects of the excitation, and were run for 250 ps. The last frame of each of these simulations was used as a starting point for the final simulations. In these simulations, the dihedral potentials were applied again, together with the ground-state atomic charges. Each simulation was performed for 3 ns. These simulations, denoted by pR, were performed to determine the effects of isomerization on the stability of the protein.

All simulations were performed in a rectangular periodic box, the volume of which was ~ 168 nm³. The system contained in total 3617 SPC water molecules,[17] including 92 crystallographic water molecules that were included explicitly. Polar and aromatic hydrogens were added to the protein. In each of the systems simulated, 6 Na^+ ions were added to compensate the net negative charge of the protein. These ions were introduced by replacing the water molecules with the highest electrostatic potential. This was done in an iterative fashion, that is, after each water molecule was replaced with an ion the electrostatic potential was recalculated. The final system contained 12,663 atoms. Prior to the pG and pR simulations, the structures were energy minimized for 200 steps, using a steepest-descent algorithm. Subsequently, these structures were simulated for 40 ps with harmonic position restraints on all protein atoms (force constant of 1.0×10^3 kJ mol^{-1} nm^{-2}) for an initial equilibration of the water molecules. All simulations were run at constant temperature and pressure, by weak coupling to an external bath[18] ($\tau_T = 0.1$ *ps* and $\tau_p = 1.0$ ps). The LINCS algorithm[19] was used to constrain bond lengths within the protein, allowing a time step of 2 fs. The SETTLE algorithm[20] was used to constrain the geometry of the water molecules. A twin-range cutoff method was used for nonbonded interactions. Lennard–Jones and Coulomb interactions within 1.2 nm were calculated at every timestep, whereas Coulomb interactions between 1.2 and 1.8 nm were calculated every 10 steps. All simulations were performed using the GROMACS simulation package[21] together with the GROMOS96 force field.[22] For this size system, we could simulate approximately 0.5 ns per day on an alpha 663-MHz processor. The generation of additional parameters required to model the chromophore is described below.

Chromophore Forcefield

The atomic charges were estimated by fitting to the charge density of the chromophore in vacuo, calculated semiempirically. These computations were performed using the MOPAC program[23] with the PM3 Hamiltonian.[24] The ESP charge fitting procedure[25] was used to derive the atomic charges. The charges were also calculated with the ADF program[10] using the multipole-derived charges procedure.[26] In this procedure, the total charge is distributed per atom in such a way that the partial atomic charges reproduce the atomic multipoles up to the quadrupole. Both approaches yielded similar charge distributions. The average and largest atomic charge variations found were 0.15 and 0.23 e, respectively. For use in the simulation, the quantum mechanically derived charges were slightly adapted to match similar fragments in the GROMOS96 force field.[22] The final charges are listed in Table 1. The excited-state partial charges were obtained from a configuration interaction calculation in which the excited state is modeled as a superposition of singly excited Slater determinants (CIS). These computations were performed using the Gaussian94 software package.[27] Dihedral parameters, which model the rotation of the conjugated bonds *a, b, c,* and *d* (Fig. 1), were obtained as follows. First, 500,000 chromophore conformations were generated by randomly varying the four dihedral angles. The energy (E^{PM3}) of each of these conformations was then calculated semiem-

TABLE I. Partial atomic charges of the chromophore in the ground state (pG), excited state (p*), deprotonated red-shifted state (pR), and protonated red-shifted state (pR-H)

Atom	pG	p^*	pR	pR-H
$S\gamma$	-0.30	-0.32	-0.20	0.00
C1	0.40	0.15	0.40	0.27
O1	-0.30	-0.43	-0.40	-0.27
C2	-0.58	-0.37	-0.40	-0.20
H2	0.33	0.23	0.10	0.10
C3	0.05	-0.20	0.20	0.00
H3	0.15	0.14	0.10	0.10
C1$'$	-0.15	-0.10	-0.30	-0.10
C2$'$	-0.14	-0.10	-0.14	-0.10
H2$'$	0.14	0.15	0.14	0.10
C6$'$	-0.14	-0.10	-0.14	-0.10
H6$'$	0.14	0.15	0.14	0.10
C3$'$	-0.40	-0.30	-0.34	-0.14
H3$'$	0.13	0.20	0.14	0.14
C5$'$	-0.40	-0.30	-0.34	-0.14
H5$'$	0.13	0.20	0.14	0.14
C4$'$	0.40	0.40	0.50	0.10
O4$'$	-0.46	-0.40	-0.60	-0.25
H4$'$				0.25

Atom names are as given in Figure 1(a).

Fig. 3. Frontier orbitals of the *p*-coumaric acid chromophore in vacuo viewed from the top. The spheres represent the atomic p_z orbitals. The relative sizes of the atomic orbitals indicate how much the respective orbitals contribute to the molecular orbital. Upon excitation, an electron is transferred from the HOMO (**a**) to the LUMO (**b**). The arrow indicates the direction of the transition dipole moment associated with that excitation.

pirically. From this energy, the GROMOS96 energy due to all other interactions was subtracted. By performing a multidimensional least-squares fit of four force field dihedral functions ($V_i(\phi_i) = k_i[1 + \cos(n\phi_i - \phi_{i0}]$, where $i = \{a, b, c, d\}$, $n = 2$, and $\phi_{i0} = \pi$) to the resulting 5-D dataset (i.e., $\{a, b, c, d, E\}$, and $E = \Sigma_i V_i$), the required dihedral parameters (k_i) were obtained.

RESULTS

Photon Absorption

The frontier molecular orbitals of the isolated chromophore are shown in Fig. 3, as viewed along the z-axis of the molecule (i.e., perpendicular to the molecular plane). The spheres represent the atomic p_z orbitals that compose the frontier molecular orbitals. The size of the atomic p_z orbitals indicates the contribution of the individual orbitals to the total molecular orbital. Because the molecular orbitals are composed entirely of overlapping p_z atomic orbitals, located on different nuclear centers in the chromophore, they are highly conjugated. The probability density of the electrons occupying each of these orbitals is distributed over the entire chromophore. In the electronic ground state of the chromophore, the highest occupied molecular orbital (HOMO; Fig. 3) is occupied by an electron pair (two electrons with antiparallel spins). Upon absorption of a photon, one of the two electrons is excited to the lowest unoccupied molecular orbital (LUMO; Fig. 3). In vacuum, the electronic transition dipole moment of this excitation is 8.74 D. The arrow in Figure 3 shows its direction. The absorption wavelength of the isolated chromophore was calculated to be 400 nm.

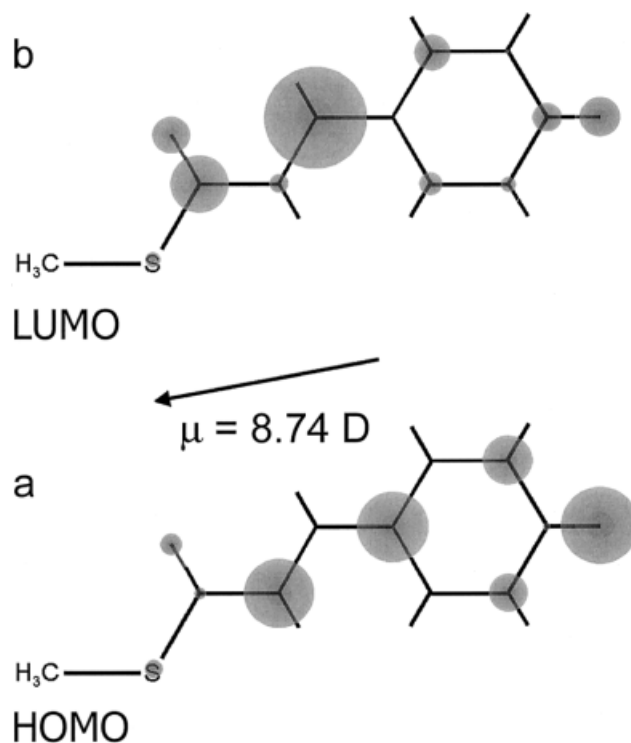Inside the protein [Fig. 1b], the calculations show that excitation no longer involves a simple transition between two well-defined chromophore orbitals. Instead, one of the electrons is promoted to an orbital that is a superposition of the chromophore's LUMO and the LUMO of an arginine residue (Arg52), stacked on top of the chromophore. This situation is shown schematically in Fig. 4. Again, the atomic orbitals that compose the molecular orbitals are indicated. As before, the size of the atomic p_z orbitals indicates their contribution to the molecular orbital. As evident in this graphical representation, some of the negative charge on the chromophore is transferred to the guanidium moiety of the Arg52 residue upon excitation inside PYP. The protein environment lowers the energy of the absorption, with the calculated absorption wavelength of the chromophore rising from 400 nm in vacuo to 442 nm (experiment 446 nm). Inside PYP, the transition dipole moment is 4.78 D. The direction of the transition dipole is indicated by the arrow in Figure 4.

An important effect of the excitation is that the barriers to rotation of the dihedrals in the tail of the chromophore become considerably lower. This is illustrated in Fig. 5. The panels in Figure 5 show a projection of both the ground and excited-state potential energy surfaces of the chromophore onto the four dihedral angles (for a definition, see Fig. 1). These curves were obtained by performing TDDFT calculations on an isolated chromophore with different conformations of the tail region. Dihedrals *a* and *b* are affected most by the photon absorption with the

LUMO_PCA + LUMO_Arg
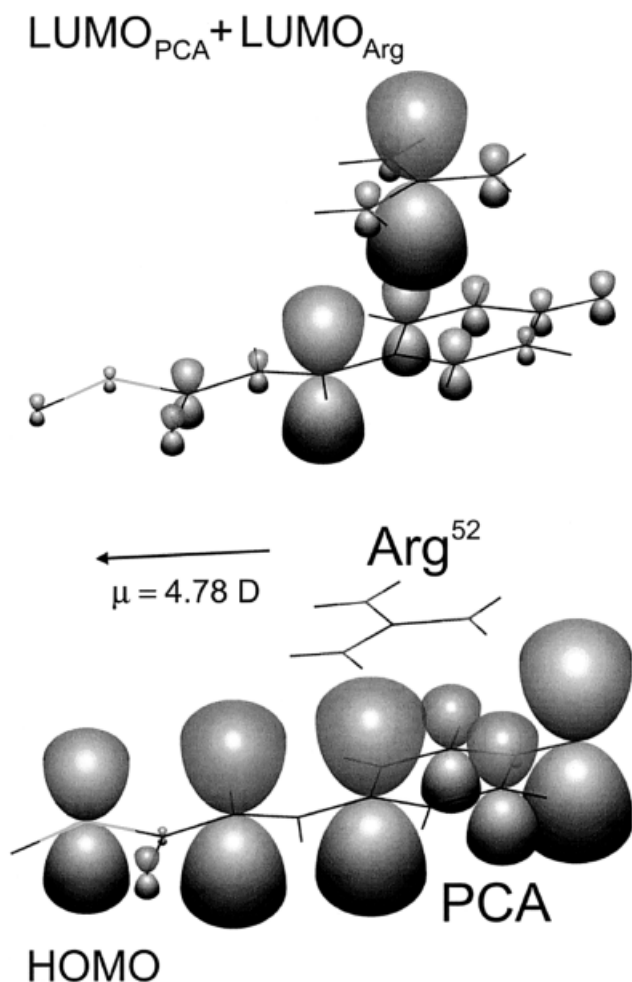
Arg^{52}

$\mu = 4.78$ D

PCA

HOMO

Fig. 4. Contribution of atomic p_z orbitals to the HOMO of the chromophore and the linear combination of the LUMO of the chromophore and the arginine (Arg[52]) in the protein. This illustrates the transfer of negative charge to the guanidium group of Arg[52] when the chromophore is embedded in PYP.

barrier to rotation significantly lower in the excited state than in the ground state. Dihedrals *c* and *d* are also affected but to a lesser extent. This observation is discussed in more detail later.

Photoisomerization

To reproduce the primary effects that excitation has on the system, a simulation was performed in which the excited-state atomic partial charges (Table 1) were applied and the dihedral potentials, modeling the rotations of the four chromophore dihedral angles, were temporarily set to zero. This is in effect a first-order approximation to the excited state (p*). Alternatively, the data shown in Figure 5 could have been used to construct excited-state dihedral potential functions. This was not done for two reasons. First, the isomerization involves multiple energy surfaces and would therefore have required explicit surface hopping[28] to treat realistically. Second, as the equilibrium geometry of the chromophore does not change upon excitation (Fig. 5; the ground and excited-state minima are the

same), the precise height of the barrier will only effect the rate of the observed conformational changes. The starting configuration for this simulation was taken from the ground-state pG simulation after 4 ns (see Materials and Methods). During the barrier-free period, dihedrals *a* and *b* (Fig. 1) rotated out of the plane by 90°, resulting in a highly distorted chromophore conformation. This is shown in Fig. 6, in which the four dihedral angles are plotted versus time. In the PYP ground-state (pG) simulation, the chromophore remains planar. After lowering the potential barriers and applying the excited-state charges, dihedrals *a* and *b* adopt values halfway between a *trans*-to-*cis* isomerization and remain stable in this transition state.

After a short period of evolution (250 ps), the ground-state atomic partial charges and dihedral potentials were reapplied. This period was chosen for convenience. No attempt was made to incorporate quantum dynamics. As is evident from Figure 6, the chromophore then smoothly isomerized further to a conformation in which dihedrals *a* and *b* are approximately 0°, corresponding to the *cis* conformation. The difference in the conformation of the chromophore before and after isomerization is shown in Fig. 7. As can be seen, the *cis* conformation, obtained from the simulations, closely resembles the ground-state *trans* conformation. In particular, the orientation of the chromophore with respect to residues Tyr42 and Glu46 is little changed. This structure closely resembles the pR X-ray structure, obtained by Perman et al.[6], using Laue diffraction techniques. The significance of the similarity is difficult to judge, especially as Genick et al. using X-ray diffraction at low temperature obtained an alternative structure of the pR intermediate.[29] Snapshots of the isomerization process observed in our simulation are shown in Fig. 8. These illustrate that the chromophore ring does not rotate out of the plane during isomerization.

The excited-state simulation was repeated a total of five times. The starting configurations for each simulation were taken at regular intervals from the reference ground-state simulation. In two of these simulations, a successful isomerization was observed. In the other three simulations, however, the chromophore remained close to its ground-state conformation (i.e., bond *b trans*; Fig. 1) throughout the barrier-less period. Reapplying the ground-state potentials and partial atomic charges thus resulted in a stable ground-state conformation.

Energy profiles corresponding to the isomerization process are plotted in Fig. 9. These profiles were obtained by TDDFT calculations on an *isolated* chromophore, using the same procedure as described previously. The conformations of that chromophore were taken from successive frames of the isomerization simulation. The energy as a function of the observed isomerization pathway is given for the ground state and for the first two electronic excited states. The reaction coordinate ξ represents the progress of the isomerization, as observed in the isomerization simulation: At ξ = 0.0, the chromophore is in its ground-state conformation (Fig. 7, pG, and Fig. 8, the leftmost structure), and at ξ = 1.0 the chromophore is in the red-shifted state conformation (Fig. 7, pR, and Fig. 8, the rightmost
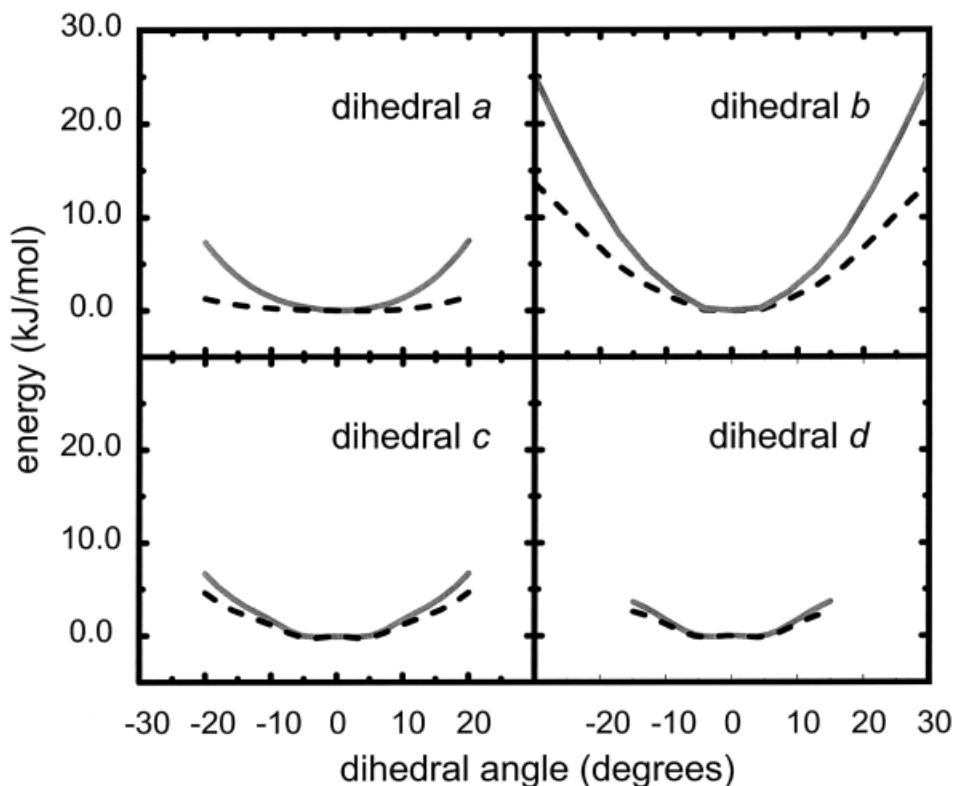
Fig. 5. Projection of the potential energy hypersurface onto the four dihedral angles in the tail of the chromophore. Solid lines correspond to the ground state. Broken lines correspond to the excited state (π, π^*).

structure). ξ thus represents the combined rotation of the four dihedral angles in the tail of the chromophore that lead to isomerization. The profiles show a number of avoided crossings. At an avoided crossing, two potential energy surfaces approach each other, but do not cross.[30]

The ground-state curve (solid line in Fig. 9) represents the chromophore when all bonding molecular orbitals are occupied by an antiparallel electron pair. The process of excitation results in one electron being promoted from the bonding HOMO orbital (Fig. 3) to the LUMO orbital. The excited state that results from this $\pi \rightarrow \pi^*$ transition is represented by the second excited-state curve (dotted line in Fig. 9). The first excited-state curve (broken line in Fig. 9) represents a state in which one electron is excited from a doubly occupied nonbonding orbital localized on the phenolate oxygen to the antibonding LUMO π orbital (Fig. 3). The probability of this $n \rightarrow \pi^*$ transition is zero if the chromophore is planar. For this reason, the first excited state is not expected to be significantly populated during excitation.

At $\xi = 0.38$, the curves of the $\pi \rightarrow \pi^*$ state and the $n \rightarrow \pi^*$ state come close but do not intersect. In the neighborhood of such an avoided crossing, electronic and nuclear motion become strongly coupled [31]. In this case, so called *nonadiabatic* transitions, in which the system undergoes a radiationless transition from one electronic state into another, can in principle occur. At $\xi = 0.38$, the system can undergo a transition from the second excited-state poten-

tial energy surface (dotted line) to the first excited-state surface (broken line). If this transition takes place, the system will encounter another avoided crossing, located near $\xi = 0.45$. This provides an opportunity to undergo another radiationless nonadiabatic transition between the first ($n \rightarrow \pi^*$) excited-state potential energy surface (broken line) and the ground-state surface (solid line in Fig. 9).

The nonadiabatic transitions outlined above yield an isomerization potential energy profile that is a combination of the ground and the first two excited states. This effective potential is represented by the long broken line in Figure 9. The barrier on this effective isomerization profile is considerably lower than the corresponding barrier on the ground-state energy surface, making isomerization possible.

Red-Shifted State Dynamics

During isomerization, the hydrogen bonding network that stabilizes the chromophore in the ground state (Fig. 7, pG) is temporarily distorted. The hydrogen bond between the phenolate group of the chromophore and the side-chain of Tyr42 remains intact but the hydrogen bond with Glu46 is lost, with the carboxylate moiety of Glu46 instead interacting with the phenol oxygen atom of Tyr42. After isomerization, the original hydrogen bonding network, in which both Tyr42 and Glu46 donate a hydrogen bond to the phenolate group of the chromophore, is quickly restored, as shown in Figure 7 (pR). To investigate the effect
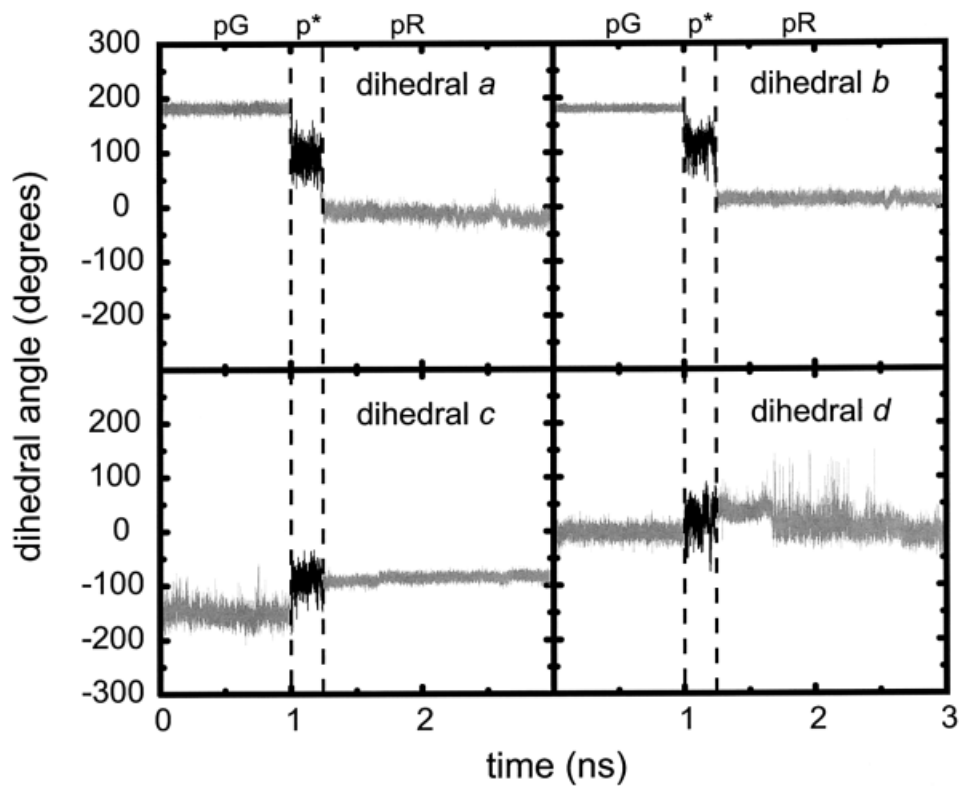
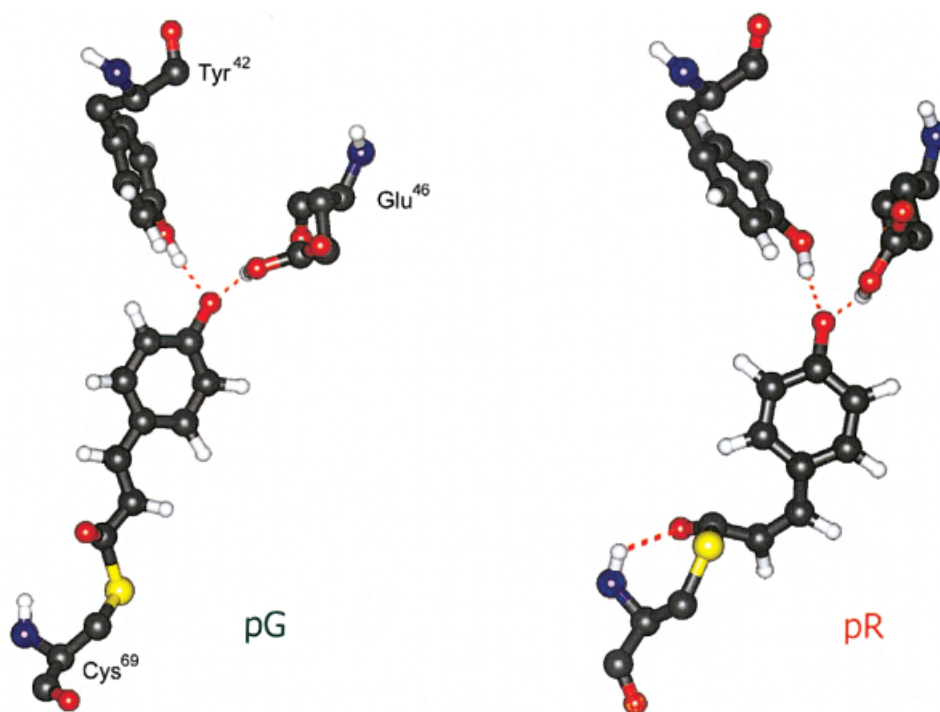Fig. 6.   Evolution of dihedrals *a, b, c*, and *d*.

Fig. 7.   Conformations of the chromophore before (pG) and after (pR) photoisomerization.

of the isomerization on the stability of the protein, the root mean square deviation (RMSD) of the backbone with respect to the starting structure was monitored before, during, and after isomerization. No indication that isomerization destabilized the protein up to 3 ns after the isomerization was observed.
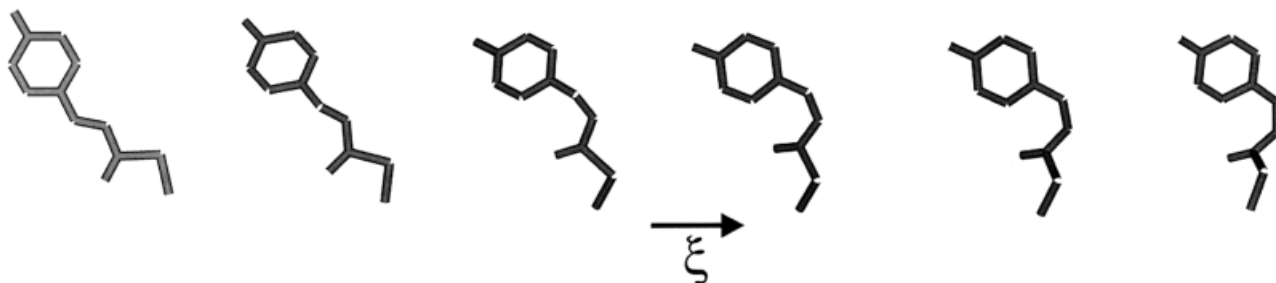
Fig. 8. Snapshots from the trajectory, illustrating the isomerization process, and showing the evolution from the *trans* configuration (left) to the *cis* configuration (right). The reaction coordinate ξ represents the progress of the reaction. ξ thus represents the combined rotation of the dihedral angles in the tail of the chromophore that lead to isomerization.
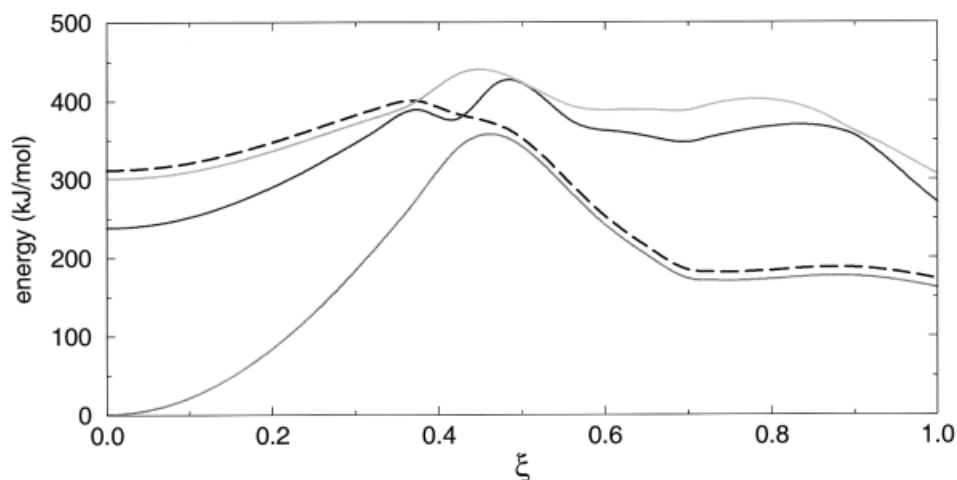

Fig. 9. Isomerization curves in the electronic ground state (solid line), the first electronically excited state ($n \rightarrow \pi^*$; broken line), and the second excited state ($\pi \rightarrow \pi^*$; dotted line) of the isolated chromophore. The long broken curve represents the effective isomerization profile. The reaction coordinate ξ (see Fig. 8) represents the progress of the isomerization. At ξ = 0 the chromophore is in the *trans* configuration and at ξ = 1 it is in the *cis* configuration. ξ thus represents the combined rotation of the dihedral angles in the tail of the chromophore that lead to isomerization.

DISCUSSION

Photon Absorption

Photon absorption by the chromophore inside PYP is believed to be the first step in the signal transduction mechanism.[5,6] The protein environment causes a red shift in the absorption frequencies of the chromophore. The isolated chromophore has an absorption maximum in the UV region of the spectrum calculated to be around 400 nm, while it absorbs blue light at 442 nm if it is buried inside PYP. The guanidium group of Arg52, located just above the chromophore, has the predominant effect on the absorption characteristics. When this guanidium group is oriented parallel with respect to the chromophore (as in Fig. 4), a charge transfer takes place upon absorption. This means that during the absorption part of the negative charge on the chromophore is transferred onto the positively charged guanidium group. The orbital that becomes partially occupied in this case is a superposition of atomic p_z orbitals located on both the chromophore and the guanidium group of Arg52. In the pG simulations, the parallel orientation of both groups occurs 50% of the time with the planes of the groups alternatively oriented paral-

lel and perpendicular with respect to each other. Excitation of the chromophore in the antistacked conformation (i.e., the planes oriented perpendicular) does not result in charge transfer. The TDDFT calculations predict a difference of approximately 20 nm in the absorption wavelength of PYP between the stacked and antistacked conformations and show that the guanidium group of Arg52 may tune and broaden the action spectrum of PYP.

Photoisomerization

The second step in the signal transduction process is proposed to be the rapid isomerization of the chromophore.[5,6] Our results suggest that upon photon absorption not only is there a considerable reduction in the energy barrier to isomerization but the protein favors isomerization by stabilizing an intermediate or transition state. In the ground state, only the HOMO is doubly occupied by electrons; the LUMO is empty. The HOMO is also highly conjugated. The stabilization associated with that conjugation is most favorable if the overlap of the atomic p_z orbitals, which contribute to the conjugated molecular orbital, is optimal, that is, when the chro-

mophore is planar. Therefore, rotation of the dihedrals in the tail of the chromophore is severely hindered in the ground state. In the excited state, both the HOMO and LUMO are singly occupied. The LUMO is antibonding and thus the stabilization by conjugation is less. This means that in the excited state planarity is not as favored as in the ground state. Twisting of the dihedrals in the excited state is energetically possible, as indicated by the excited-state isomerization profile (Fig. 9).

Further, the protein selectively stabilizes the transition state in a barrier-free isomerization process. The barrier does not completely vanish upon excitation and this observation strongly suggests that photoisomerization is protein assisted. The barrier to isomerization is high in the ground state (340 kJ/mol) and the chromophore remained planar in the pG simulation. In the excited state, the barrier is lower (60 kJ/mol) and in a range that can be further compensated by the protein. Immediately following absorption, the protein was observed to drive the chromophore toward the transition state in two of five attempts. During this phase, nonadiabatic transitions can occur that return the chromophore to the electronic ground state. Together, the photon and the protein efficiently drive the chromophore to a saddle-point of the ground-state potential energy surface. From there, the chromophore can slide down on either side of the saddle-point. If it slides back to its pG conformation (bond *b trans*), the photon absorption will not lead to signal transduction. This pathway accounts for the fact that the quantum yield for entering the photocycle is only 0.35.[6] On the other hand, the chromophore can also continue its path and end up in the isomerized conformation (bond *b cis*). In this case, the photon absorption results in PYP reaching the third stage of the photocycle, essential for transmitting the signal.

The above assumes that the chromophore undergoes a nonadiabatic transition from one surface to another at each avoided crossing encountered during the photoisomerization process (at $\xi = 0.38$ and $\xi = 0.45$; Fig. 9). When a system passes through a region of configuration space (i.e., the space spanned by the degrees of freedom in the system) where two electronic states are nearly degenerate, the system will evolve as a superposition of the nearly degenerate states. This is a direct consequence of the Heisenberg uncertainty relation: $\Delta E \Delta t \geq \hbar$.[32] In the current case, ΔE is the splitting between the two electronic energy surfaces in a small region of configuration space and Δt is the time the system spends in that region. As the system moves along the reaction coordinate with a certain velocity, this time interval Δt is finite, implying some degree of uncertainty in the energy of the system. Because $\hbar$ is small, the uncertainty in the energy in most cases can be neglected.

However, near avoided crossings ΔE becomes small and the uncertainty in the total energy of the system (in the order of $\hbar$) becomes comparable to the energy gap. In this case, it is no longer possible to distinguish between the two electronic states. In effect, the system becomes a superposition of both electronic states. At some time in the future, the probability of finding the system in one of the two possible states will depend on the time spent in the avoided crossing region (or, equally, on the speed of the system in that region). The relation between the speed of the system at an avoided crossing and the probability (P) to be found on either one of the potential energy surfaces may be approximated by the following equation [33]:

$$P = \exp\left[\frac{-2\pi H_{12}^2}{\hbar v \Delta F}\right], \tag{1}$$

where H_{12} is half the energy difference between the two states at the avoided crossing, ΔF the difference in the slopes of both curves at the avoided crossing, v the speed at which the system passes the avoided crossing, and $\hbar$ Planck's constant divided by 2π.

To accurately calculate the transition probabilities would require detailed simulations of the excited state. These were not performed for reasons described earlier. Nevertheless, from our barrier-less simulation we know that the chromophore moves into the transition state rapidly (within a few picoseconds; see Fig. 6). Moreover, the TDDFT calculations indicate that the energy gap between the potential energy curves is small at the avoided crossings, on the order of a few kJ/mol. Therefore, the exponent in eq. 1 will approach zero and the probability of transition will approach 1 at both avoided crossings.

With the protocol of our isomerization simulation, the removal of the dihedral potentials of the chromophore and the application of excited-state partial charges (Table I) to mimic the excited state (p*) of PYP, before instantaneously reverting to the ground-state partial charges (Table I) and potentials, we effectively model the two nonadiabatic transitions that take place during the isomerization in the excited state. To explicitly simulate the excited state would be preferable. However, the creation of a reliable excited state force field is still computationally prohibitive.

As a control, an isolated chromophore was simulated in vacuo without dihedral barriers and excited-state charges. In this simulation, dihedral *a* was flexible and did undergo rotations. Dihedral *b* remained in its *trans* configuration. No transition state-like conformation was observed. This suggests that the protein specifically channels the isomerization along a specific pathway.

Red-Shifted State Dynamics

The isomerization of the chromophore does not have an immediate impact on the stability of the protein. The simulation period was at least three orders of magnitude smaller than the period in which the system fully evolves from the red-shifted to the blue-shifted state. Nevertheless, the conformation of chromophore after isomerization is similar to the conformation before isomerization (Fig. 7). All hydrogen bonds to the protein remain intact. It is thus unlikely that the relatively small changes associated with photoisomerization directly induce conformational changes in the protein that are thought to lead to signal transduction. Instead, additional steps, such as a proton transfer to the chromophore's phenolate oxygen atom, are most likely required. This hypothesis is considered in a separate article.

CONCLUSIONS

The calculations presented here suggest that PYP selectively stabilizes the transition state in the process leading to the isomerization of the chromophore. In the electronic ground state, the internal barrier to isomerization within the protein is high. In the excited state, the barrier is considerably lowered. By stabilizing the isomerization transition state, the protein both regulates the process of isomerization and ensures a high quantum yield. The isomerization process is not accompanied by large conformational changes in the chromophore region. Moreover, isomerization itself does not appear to directly effect protein stability. Therefore, it is unlikely that the mechanical effects of isomerization are alone sufficient to cause the conformational changes in PYP that are believed, in turn, to give rise to signal transduction.

NOTE ADDED IN PROOF

Recent ab initio studies by Tamada et al.[34] have shown that the inclusion of the hydrogen bond donors Tyr42 and Glu46 when calculating the potential energy surface of the coumaric acid chromphore flattens the effective potential energy curve associated with dihedral d in the excited state significantly. Thus the assumption used in this study that there is no-barrier to rotation is more correct than might be inferred from Figure 5.

REFERENCES

1. Hellingwerf KJ, Crielaard WC, de Mattos MJT, Hoff WD, Kort R, Verhamma DT, Avignone-Rossa C. Current topics in signal transduction in bacteria. Antonie Leeuwenhoek 1998;74:211–227.
2. Pellequer JD, Wager-Smith KA, Getzoff ED. Photoactive yellow protein: a structural prototype for the three-dimensional fold of the pas domain superfamily. Proc Natl Acad Sci USA 1998;95:5884–5890.
3. Baca M, Borgstahl G, Boissinot M, Burke P, Williams D, Slater K, Getzoff E. Complete chemical structure of photoactive yellow protein: novel thioester-linked 4-hydroxyxinnamyl chromophore and photocycle chemistry. Biochemistry 1994;33:14369–14377.
4. Borgstahl GEO, Williams DR, Getzoff ED. 1.4 A structure of photoactive yellow protein, a cytosolic photoreceptor: unusual fold, active site and chromophore. Biochemistry 1995;34:6278–6287.
5. Hendriks J, Hoff WD, Crielaard W, Hellingwerf KJ. Protonation/deprotonation reactions triggered by photoactivation of photoactive yellow protein from *ectothiorodospira halophila*. J Biol Chem 1999;274:17655–17660.
6. Perman B, Šrajer V, Ren Z, Teng TY, Pradervand C, Ursby T, Bourgeois D, Schotte F, Wulff M, Kort R, Hellingwerf KJ, Moffat K. Energy transduction on the nanosecond time scale: early structural events in a xanthopsin photocycle. Science 1998;279:1946–1950.
7. Xie A, Hoff WD, Kroon AR, Hellingwerf KJ. Glu46 donates a proton to the 4-hydroxycinnamate anion chromophore during the photocycle of photoactive yellow protein. Biochemistry 1996;35:14671–14677.
8. Genick UK, Borgstahl GE, NgK, Ren Z, Pradervand C, Burke PM, Šrajer V, Teng TY, Schildkamp W, McRee DE, Moffat K, Getzoff ED. Structure of a protein photocycle intermediate by millisecond time-resolved crystallography. Science 1997;275:1471–1475.
9. Rubingstenn G, Vuister GW, Mulder FAA, Düx PE, Boelens R, Hellingwerf KJ, Kaptein R. Structural and dynamic changes of photoactive yellow protein during its photocycle in solution. Nature Struct Biol 1998;5:568–570.
10. te Velde G, Bickelhaupt FM, Baerends EJ, van Gisbergen SJA, Guerra CF, Snijders JG. Chemistry with adf. J Comput Chem 2001;22:931–967.
11. van Gisbergen SJA, Snijders JG, Baerends EJ. Implementation of time-dependent dnesity functional response equations. Comp Phys Commun 1999;118:119–138.
12. Gross EKU, Kohn W. Time-dependent density functional theory. Adv Quantum Chem 1990;21:255–291.
13. Allen MP, Tildesley DJ. Computer simulations of liquids. Oxford, UK: Oxford Science Publications; 1987.
14. Frenkel D, Smit B. Understanding molecular simulations: from algorithms to applications. New York: Academic Press; 1996.
15. van Gisbergen SJA. Molecular response property calculation using time-dependent density fuctional theory. PhD thesis, Free University, Amsterdam; 1998.
16. van Gisbergen SJA, Rosa A, Ricciardi G, Baerends EJ. Time-dependent density functional calculations on the electronic absorption spectrum of free base porphin. J Chem Phys 1999;111:2499–2506.
17. Berendsen HJC, Postma JPM, van Gunsteren WF, Hermans J. Interaction models for water in relation to protein hydration. In: Pullman B, editor. Intermolecular forces. Dordrecht: D. Reidel; 1981. P 331–342.
18. Berendsen HJC, Postma JPM, van Gunsteren WF, DiNola A, Haak JR. Molecular dynamics with coupling to an external bath. J Chem Phys 1984;81:3684–3690.
19. Hess B, Bekker H, Berendsen HJC, Fraaije JGEM. LINCS: A linear constraint solver for molecular simulations. J Comput Chem 1997;18:1463–1472.
20. Miyamoto S, Kollman PA. SETTLE: An analytical version of the SHAKE and RATTLE algorithms for rigid water models. J Comput Chem 1992;13:952–962.
21. van der Spoel D, Hess B, Feenstra KA, Lindahl E, Berendsen HJC. GROMACS user manual, Version 2.0. Groningen, The Netherlands; 1999. http://md.chem.rug.nl/~gmx.
22. van Gunsteren WF, Billeter SR, Eising AA, Hünenberger PH, Krüger P, Mark AE, Scott WRP, Tironi IG. Biomolecular simulation: GROMOS96 manual and user guide. Groningen, The Netherlands; BIOMOS b.v. Zürich; 1996.
23. Stewart JJP. Mopac version 2000. Tokyo; Fujitsu; 1999.
24. Stewart JJP. Optimization of parameters for semiempirical methods I. methods. J Comput Chem 1989;10:209–221.
25. Besler BH, Merz KM Jr, Kollman PA. Atomic charges derived from semiempirical methods. J Comput Chem 1990;11:431–439.
26. Swart M, van Duijnen PT, Snijders JG. A charge analysis derived from an atomic multipole expansion. J Comput Chem 2000;22:79–88.
27. Frisch, MJ, Trucks GW, Schlegel HB, Gill PMW, Johnson BG, Robb MA, Cheeseman JR, Keith TA, Petersson GA, Montgomery JA, Raghavachari K, Al-Laham MA, Zakrzewski VG, Ortiz JV, Foresman JB, Ciosloswki J, Stefanof BB, Nanayakkara A, Challacombe M, Peng CY, Ayala PY, Chen W, Wong MW, Andres JL, Replogle ES, Gomperts R, Martin RI, Fox DJ, Binkley JS, Defrees DJ, Baker J, Stewart JJP, Head-Gordon M, Gonzalez C, Pople, JA. Gaussian 94, Revision A.1. Pittsburgh, PA: Gaussian Inc.; 1995.
28. Tully JC. Molecular dynamics with electronic transitions. J Chem Phys 1990;93:1061–1071.
29. Genick UK, Soltis SM, Kuhn P, Canestrelli IL, Getzoff ED. Structure at 0.85 Å resolution of an early protein photocycle intermediate. Nature 1998;392:206–209.
30. Atkins PW. Physical chemistry, Fourth Ed. Oxford, UK: Oxford University Press; 1990.
31. Köppel H, Domcke W, Cederbaum LS. Multimode molecular dynamics beyond the Born-Oppenheimer approximation. Adv Chem Phys 1984;57:59–246.
32. Gasiorowicz S. Quantum physics. New York: Wiley; 1996.
33. Zener C. Non-adiabatic crossing of energy levels. Proc Roy Soc London A 1932;137:696–702.
34. Yamada A, Yamamoto S, Yamato T, Kakitani T. Ab initio MO study on potential energy surfaces for twisting around C7-C8 and C4-C7 bonds of coumaric acid. J Mol Struc: THEOCHEM 2001;536:195–2001.